Control and Cybernetics

vol. **27** (1998) No. 2

Structural optimization with a non-smooth buckling load criterion

by

J. Folgado and H. Rodrigues

IDMEC - Instituto Superior Tecnico,
Av. Rovisco Pais, 1096 Lisboa, Portugal

Abstract: This work addresses problems in optimal design of structures with a non-smooth buckling load criterion and in particular applications in layout design of plate reinforcements using a material based model and thickness beam optimization problems. Starting with the formulation of the linearized buckling problem, the optimization problem is formulated and the optimal necessary conditions are derived. Considering the possibility of non-differentiability of the objective function, the optimal necessary conditions are stated in terms of generalized gradients for non-smooth functions. The importance of the obtained result is analyzed and directional derivatives of the critical load factor obtained from the generalized gradient set definition, are compared with forward finite difference approximations. Optimization applications, to test the developments done, are presented. They are performed using a mathematical programming code, the Bundle Trust Method, which addresses the non-smoothness of the problem.

Keywords: structures, homogenization, buckling, non-smooth optimization

1. Introduction

Material based models have been widely applied to the problem of topology optimization of structures (Bendsoe and Mota Soares, 1993) and to the layout design of plate and shell reinforcements (see e.g., Suzuki and Kikuchi, 1991, and Soto and Diaz, 1993). Initially, these applications dealt with compliance based criteria but lately various extensions have been presented namely to the optimal control of natural frequencies (see e.g., Diaz and Kikuchi, 1993) and buckling loads (see e.g. Neves et al., 1995).

The model presented in this work uses a laminate plate theory and a linearized buckling model and the objective is to find the optimal material distribution, simulating the plate reinforcement in the exterior laminas, that maximizes

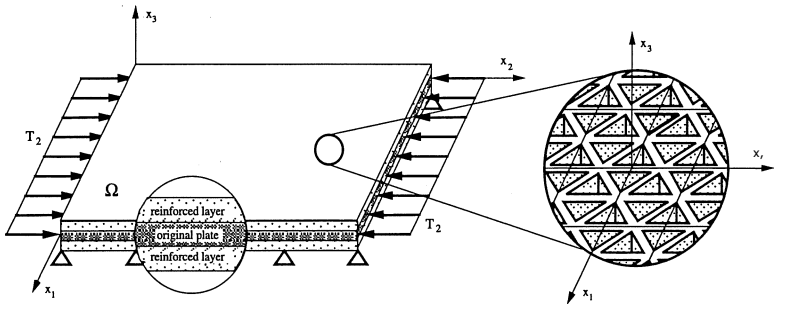

Figure 1. Plate optimization model

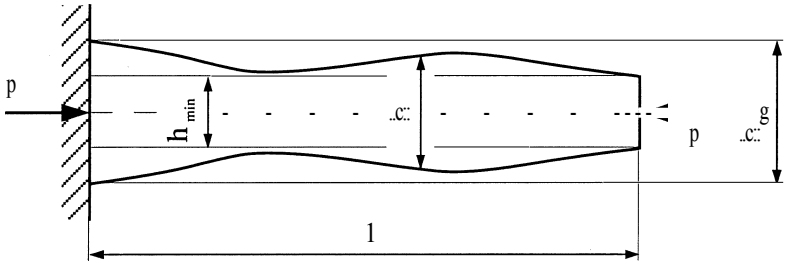

Figure 2. Beam optimization problem

the plate lowest buckling load. The plate cross section is symmetric and obtained by joining different layers of material where the internal layers represent the original plate and are fixed in terms of design. The outer layers are made of a porous material with variable relative density obtained by the introduction, at the material "microstructure" level, of small voids. These design layers act like micro-perforate plates (see Fig. 1). The microstructure of this material is assumed to be locally periodic and the dimension of the voids characterizing the relative density, μ, defines the reinforcement material distribution at each point. Regions with high-density values indicate reinforcement while low values indicate no reinforcement. The total amount of material available is constrained. Based on the linearized plate buckling equations the buckling load is computed numerically by a finite element approximation of the problem.

The thickness beam optimization problem is also considered in order to maximize the lowest buckling load. In this case the design variable is the thickness of the beam, which can vary between a minimum and a maximum value. The amount of material available to the beam is constrained by an upper bound. The linearized beam buckling equations are derived and solved numerically using a finite element approximation.

The main difficulty in structural optimization with a buckling load criterion

derives from the fact that multiple eigenvalues are non-smooth with respect to the design variables. Considering this possibility the optimal necessary conditions are stated in terms of generalized gradients (Rodrigues et al., 1995) and solved using the mathematical programming code Bundle Trust Method (Schramm and Zowe, 1992), meant for non-smooth optimization problems.

Otherwise stated, summation convention is assumed, Greek indices vary from 1 to 2 while Latin indices vary from 1 to 3 and bold letters identify tensors.

2. Linearized buckling problem

2.1. General case

The linearized buckling problem can be obtained by introducing a displacement perturbation u^1 to the fundamental linear elastic displacement field u^0, that is $u = u^0 + a u^1$ (Novozhilov, 1953). For the general 3D case the equations can be stated as:

Find ,\ (critical load factor) and u^1 (mode) satisfying the boundary kinematics conditions and satisfying,

$$\int_{\Omega} [E_{ijkl} f_{kl}(u1) E_{ij}(ou1)]\, d\Omega - A \int_{\Omega} \left[E_{ijkl} E_{kl}(u^0) \cdot \cdot \right] d\Omega = 0, \ \forall 8u^1 \text{ admissible} \tag{1}$$

In the previous problem u^0 (fundamental displacement) is the solution of the linear elasto-static problem,

find u^0 satisfying the kinematics boundary conditions and solving,

$$\int_{\Omega} [E_{ijkl} E_{kl}(u^0) E_{ij}(8u^0)]\, d\Omega = \int_{\Gamma} (f_i 8u?)\, d\Gamma + \int_{\Omega} t_i 8u?\, d\Omega, \ \forall ou^0 \text{ admissible} \tag{2}$$

where an admissible displacement field is such that, u^0, u^1 are regular enough and u? = ui, uf = 0 on ru,•

2.2. Plate problem

If one excludes the possibility of local buckling at the material "microstructure" level, the main hypothesis of homogenization methods, stating that the local displacement fields are periodic at the microstructure level due to the local periodicity of the microstructure, is valid (Neves et al., 1995) and the material properties are given by (see Guedes and Kikuchi, 1990)

$$E f J_{km} = \frac{1}{|Y|} \int_{Y} \left(E_{ijkl} - E_{ijpq} \frac{\partial \chi^{km}}{\partial y_q} \right) dY \tag{3}$$

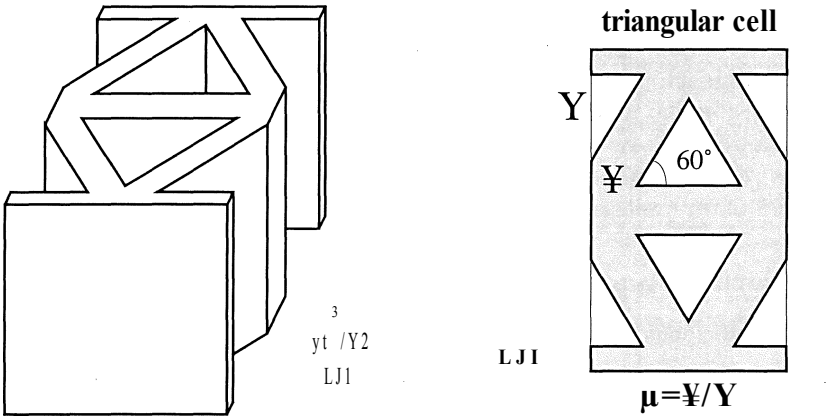

Figure 3. Microstructure

In the previous expression, IYIis the volume of the cell characterizing the microstructure, ¥ is the solid part of the cell and x^{km} is solution of the elastostatic problem at the cell level,

$$\int_{¥} E_{ijpq}\left(\frac{\partial x^{m}_{p}}{\partial Y_{q}} - \frac{\partial v_{i}}{\partial Y_{j}}\right) dY = \int_{¥} E_{ijkm}\frac{\partial v_{i}}{\partial Y_{j}}\, dY, \quad \forall v \in V¥, \tag{4}$$

with V¥{v(y), defined in¥, v is regular enough; v(y)Y- periodic}.

To obtain homogeneous material properties as an explicit function of the material density μ, the above problems are solved for several distinct values of μ and a polynomial interpolation is then used to compute property values for intermediate values.

Note that due to the cell symmetries (see Fig. 3) the material has transverse isotropy.

For the plate model we impose that in each lamina the normal transversal stress must be zero ($\sigma_{33} = 0$), which implies the constitutive relations,

$$\sigma_{\alpha\beta} = E^{*}_{\alpha\beta\gamma\delta}\varepsilon_{\gamma\delta}, \quad \sigma_{\alpha 3} = 2E_{\alpha 3 \gamma 3}\varepsilon_{\gamma 3}, \quad E^{*}_{\alpha\beta\gamma\delta} = E_{\alpha\beta\gamma\delta} - \frac{E_{\alpha\beta 33}E_{33\gamma\delta}}{E_{3333}} \tag{5}$$

Assuming now the following displacement field (Mindlin plate),

$$\begin{aligned} u_{\alpha}(x_1,x_2,x_3) &= u_{\alpha}(x_1,x_2) - x_3\theta_{\alpha}(x_1,x_2) \\ u_3(x_1,x_2,x_3) &= u_3(x_1,x_2) \end{aligned} \tag{6}$$

we obtain the strain components,

$$\epsilon_{\alpha\beta} = \frac{1}{2}\left(\frac{\partial u_{\alpha}}{\partial x_{\beta}} + \frac{\partial u_{\beta}}{\partial x_{\alpha}}\right) - x_3 \cdot \frac{1}{2}\left(\frac{\partial \theta_{\alpha}}{\partial x_{\beta}} + \frac{\partial \theta_{\beta}}{\partial x_{\alpha}}\right) =$$

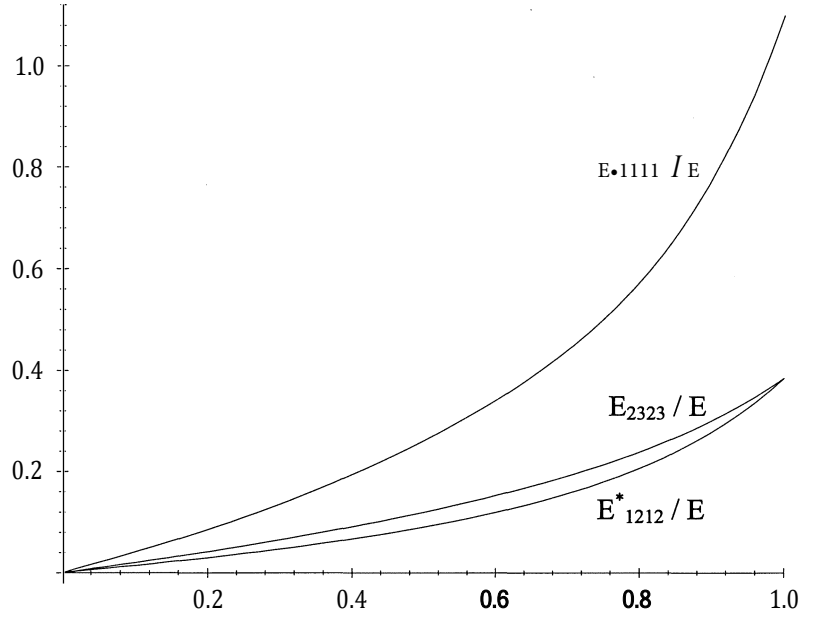

Figure 4. Material properties function of relative density

$$
\begin{aligned}
&= \epsilon^0_{\alpha\beta}(\mathbf{u}) - x_3 \cdot \kappa_{\alpha\beta}(\eta) \\
\epsilon_{\alpha 3} &= \frac{1}{2}\left(\frac{\partial u_3}{\partial x_\alpha} - \beta_\alpha\right) = \epsilon_{\alpha 3}(u_3, \eta)
\end{aligned} \tag{7}
$$

Based on these strain components, the constitutive relation (5), and by integrating along the plate thickness, the linearized plate buckling problem can be stated as (see e.g., Kam and Chang, 1992):

Find U§, 7)[1] satisfying the boundary kinematics conditions and load factor >. solving,

$$
\begin{aligned}
&\textit{in}\ \text{Da,6,61i:„a(rJ}^1)\,\text{lia6(0rJ}^1) + 4\text{Sa3,3E}_1\text{3(u⅓7)}^1)\text{Ea3(8u⅓07)}^1)]\ dD - \\
&- A \int_{\text{Vau}^1/2,07]^1} \left[4a,a,6\tilde{E},6(u^0) \frac{8u\S}{8Xa} \frac{88u\S}{X6} + Da,a,6\tilde{E},6(u^0) \frac{8(3j}{8Xa} \frac{88(3j}{X6} \right] dD = 0,
\end{aligned} \tag{8}
$$

where u^0 is solution of the elasto-static problem,

find u^0 satisfying the boundary kinematics conditions and solving

$$
\int_\Omega \left[A_{\alpha\beta\gamma\delta}\epsilon^0_{\gamma\delta}(\mathbf{u}^0)\epsilon^0_{\alpha\beta}(\delta\mathbf{u}^0)\right] d\Omega =
$$

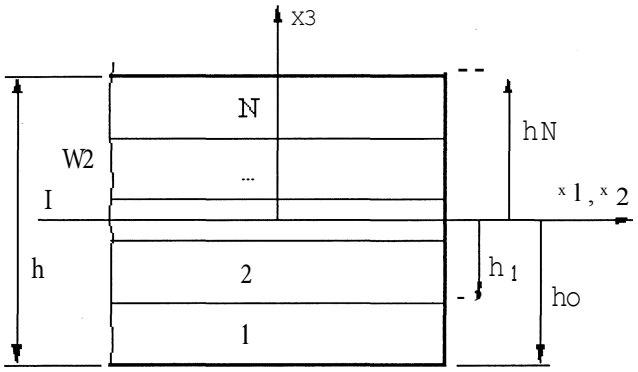

Figure 5. Laminate topology

$$= \int_{\Omega} (p_\alpha \delta u_\alpha^0) d\Omega + \sum_{\alpha=1}^{2} \int_{\Gamma_{T_\alpha}} T_\alpha \delta u_\alpha^0 d\Gamma, \ \forall \delta \mathbf{u}^0 \tag{9}$$

In the previous equations and for the geometry of the (symmetric) laminate (see Fig. 5), the tensors A, D and S are defined as (Vinson and Sierakowski, 1987),

$$\begin{aligned}
A_{\alpha\beta\gamma\delta} &= \int_{-h/2}^{h/2} E^*_{\alpha\beta\gamma\delta} dz = \sum_{j=1}^{N} (h_j - h_{j-1}) \cdot E^{*(j)}_{\alpha\beta\gamma\delta} \\
D_{\alpha\beta\gamma\delta} &= \int_{-h/2}^{h/2} (x_3)^2 \cdot E^*_{\alpha\beta\gamma\delta} dz = \frac{1}{3} \cdot \sum_{j=1}^{N} (h_j^3 - h_{j-1}^3) \cdot E^{*(j)}_{\alpha\beta\gamma\delta} \\
S_{\alpha 3\gamma 3} &= \int_{-h/2}^{h/2} f(x_3) \cdot E_{\alpha 3\gamma 3} dz = \\
&= \frac{5}{4} \cdot \sum_{j=1}^{N} \left[h_j - h_{j-1} - \frac{4}{3h^2} (h_j^3 - h_{j-1}^3 \right] \cdot E^{*(j)}_{\alpha 3\gamma 3}
\end{aligned} \tag{10}$$

2.3. Plane beam case

For a beam and considering the displacements in the x_1 - x_3 plane only, we impose the constitutive relations

$$0\text{-}11 = EE11, \quad 0\text{-}13 = 2GE13 = G\text{—}y1 \tag{11}$$

Assuming the following displacement field (Timoshenko beam theory),

$$\begin{aligned}
u_1(x_1, x_3) &= u_1(x_1) - x_3 \beta(x_1) \\
u_3(x_1, x_3) &= u_3(x_1)
\end{aligned} \tag{12}$$

we obtain the strain components,

$$\epsilon_{11} = \frac{8u_1}{uX_1} - X3 \cdot \frac{8/3}{uX_1} = E^0_{11}(u_1) - X3 \cdot {}'''_{11}(\beta)$$

$$\epsilon_{13} = 2\left(\frac{8u_3}{8x_1} - /3\right) = El3(u3,/3) \Rightarrow 'Yl = \frac{8u3}{8x_1} - /3 \tag{13}$$

The next developments will only consider concentrated applied forces at $x_1 = x_1$. So, based on the previous strain components, the constitutive relation (11), and integrating along the beam cross section the elasto-static problem can be stated as,

find u^0, β° satisfying the kinematic boundary conditions and solving

$$\int_0^L [EAE1(u)E1(8u) + EI'''_{11}(/3°)'''11(8(3°)+$$

$$+GAs--Yl(ug, /3°h1(8ug, 8(3°)]dx_1$$

$$= \sum_{i=1,3} \bar{T}i8u?(x_1 = x1)\, Vou^0, 8\beta^\circ \tag{14}$$

where A, I and As represent the cross-area, second moment of area and effective shear area, respectively. Note that in the last equation the summation (applied forces) is only taken for i = 1 and i = 3.

Repeating the same procedure as done for equation (14), the linearized beam buckling problem is stated as,

find u^1, β^1 satisfying the kinematic boundary conditions and load factor $\succ$ solving

$$\int_0^L [Ehu(/31)t,_{11}(8/31) + GAs'Yl(u½, \beta^1 h1(8u½, 8/3^1)]dx1 -$$

$$- A \int_0^L [EAE^0_{11}(u_1^0)\frac{OU§}{uX_1}\frac{88u½}{uX_1} + Eh^0_{11}(u_1^0)\frac{8/3^1}{uX_1}\frac{88/3^1}{uX_1}]\, dx_1 = 0 \tag{15}$$

$$'t/8u^1, 8/3^1$$

where u^0 is the solution of problem (14) and the symmetry of the beam is taken into consideration.

2.4. Finite element model

To solve the problem computationally, the set of equations (8), (9) for the plate or (14), (15) for the beam case, are discretized by a finite element model. For the plate model an eight-node isoparametric element, with selective integration is used and for the beam problem a two-node element with reduce integration is adopted (Hughes, 1987). By means of this approximation, equations (8) and (15) can be stated symbolically as the generalized eigenvalue problem,

$$K(b)cp - .\backslash G(b, \omega)cp = 0 \tag{16}$$

In this eigenvalue problem, $\varphi = \{\varphi_i\} \in R^N$ (N equals number of degrees of freedom per node times number of nodes) represents the eigenvector or mode, $b = \{b_e\} \in R^M$ denotes the vector of design variables (relative density for the plate problem and beam thickness for the beam problem) that are assumed to be constant for each finite element. The vector $u = \{u_i\} \in R^N$ is the finite element approximation of the fundamental displacement, solution of a finite element approximation of the linear elasto-static problem (9) or (14),

$$\mathbf{K(b)u = F} \tag{17}$$

where K and G denote the stiffness and geometric matrices respectively and F the load vector. The generalized eigenvalue problem (16) is solved by the subspace iteration method using the Householder's method to solve the resultant reduced problem.

3. Optimization problem

3.1. Problem formulation

The optimal design problem is to maximize the lowest positive eigenvalue λ (critical load λ_{cr}). Assuming that the eigenvalues are strictly positive this is equivalent to minimize the maximum of the inverse of all eigenvalues. With the above notation and using the Rayleigh quotient, the optimal design problem is restated as,

$$\min_{b_e} \left(\max_{\phi \neq 0} \frac{\phi^T \mathbf{G}(\mathbf{b}, \mathbf{u}) \phi}{\phi^T \mathbf{K}(\mathbf{b}) \phi} \right) \tag{18}$$

subjected to the following constraints:

The volume constraint that bounds the total amount of material available for design (reinforcement),

$$\sum_{e=1}^{M} b_e \int_{\Omega^e} d\Omega = \bar{V} \tag{19}$$

Upper and lower bound local constraints on the design variables (material density or beam thickness)

$$0 \quad b_e \quad 1, \; e = 1, \ldots, M \tag{20}$$

and the equilibrium constraint that gives the dependence of the fundamental linear elastic displacement u on the design variable vector b

$$\mathbf{K(b)u = F} \tag{21}$$

3.2. Optimality conditions

To obtain the necessary conditions for the optimization problem stated above, let us introduce a Lagrangian associated with the problem where the pre-bifurcation equilibrium equation (21) is considered as an additional constraint,

$$L = \left(\max_{\phi \neq 0} \frac{\phi^T \mathbf{G}(\mathbf{b},\mathbf{u})\phi}{\phi^T \mathbf{K}(\mathbf{b})\phi}\right) + \mathbf{v}^T(\mathbf{K}(\mathbf{b})\mathbf{u} - \mathbf{F}) + \Lambda\left(\sum_{e=1}^{M} b_e \int_{\Omega^e} d\Omega - \bar{V}\right) + \sum_{e=1}^{M}[\eta_e^1(b_e - 1) - \eta_e^0 b_e] \tag{22}$$

In the previous Lagrangian, v is the adjoint displacement field, the Lagrange multiplier of the equilibrium equation (21), A is the Lagrange multiplier for the volume constraint (19) and η^0, η^1 are multipliers associated with the bound constraints (20). We note that in the case of multiple eigenvalues, the objective function is non-differentiable. So, let us assume that, at the optimal solution, the critical load factor has multiplicity "m" and let ϕ_i, $i = 1, \ldots, m$ be any set of m orthonormal (with respect to K) eigenvectors corresponding to the critical load factor λ_{cr}. From non-smooth optimization theory (Clarke, 1982) the optimal necessary condition is stated as OE 8bL, where 8bL identifies the Lagrangian's generalized gradient defined as (Rodrigues et al., 1995),

$$\partial_b L = co\left\{\mathbf{z}, z_e = \alpha_p \alpha_q \left(\phi_p^T \left[\frac{\partial \mathbf{G}}{\partial b_e} - \frac{1}{\lambda_{cr}}\frac{\partial \mathbf{K}}{\partial b_e}\right]\phi_q - \mathbf{v}_{pq}\frac{\partial \mathbf{K}}{\partial b_e}\hat{\mathbf{u}}\right) : \alpha \in \mathbf{R}^m, \; \|\alpha\| = 1\right\} + \mathbf{z}_0. \tag{23}$$

where "co" means the convex hull of the set.

In the above generalized gradient we have:

$\mathbf{v}_{pq}$ is the solution of the adjoint equation,

$$\mathrm{K}\mathbf{v}_{pq} = \{\phi_p : \phi_q\}, \; p, q = 1, \ldots, m, \tag{24}$$

$\mathbf{z}_0$ represents the volume and lateral constraint components of the generalized gradient,

$$\mathbf{z}_0 = \{z_{0_e}\} = \Lambda + \int_{\Omega^e} d\Omega + \eta_e^1 - \eta_e^0 \tag{25}$$

and the terms between brackets are the generalized gradient of the inverse of the critical load factor

$$\begin{aligned} \partial_b\left(\frac{1}{\lambda_{cr}}\right) &= co\left\{\mathbf{z}, z_e = \alpha_p \alpha_q \left(\phi_p^T \left[\frac{\partial \mathbf{G}}{\partial b_e} - \frac{1}{\lambda_{cr}}\frac{\partial \mathbf{K}}{\partial b_e}\right]\phi_q - \mathbf{v}_{pq}\frac{\partial \mathbf{K}}{\partial b_e}\hat{\mathbf{u}}\right) : \right. \\ &\quad \left. \alpha \in \mathbf{R}^m, \; \|\alpha\| = 1\right\} \\ &= co\{\mathbf{z} = \alpha_p \alpha_q \mathbf{z}_{pq} : \alpha \in \mathbf{R}^m, \; \|\alpha\| = 1\}. \end{aligned} \tag{26}$$

We can rewrite expression (23) as (see Seyranian et al., 1994),

$$\partial_b L = \left\{ H_{pq} \left(\phi_p^T \left[\frac{\partial \mathbf{G}}{\partial b_e} - \frac{1}{\lambda_{cr}} \frac{\partial \mathbf{K}}{\partial b_e} \right] \phi_q - \mathbf{v}_{pq} \frac{\partial \mathbf{K}}{\partial b_e} \hat{\mathbf{u}} \right) + \mathbf{z}_0 \right\} = \{ H_{pq} \mathbf{z}_{pq} + \mathbf{z}_0 \} \quad (27)$$

where $H = \{H_{pq}\}$ is a general semi-definite m x m matrix with $\mathrm{tr} H = 1$.

3.3. Optimization algoritlun - BT code

An optimization process based on the mathematical programming code, Bundle Trust Method (Schramm and Zowe, 1992), solves the previous necessary conditions. The version of the code used was BTNCLC (Outrata et al., 1991), which can handle non-convex objective functions and linear constraints. It uses quadratic programming, to solve a subproblem, which turns out to be important in the performance of the method.

To use BTNCLC the objective function, linear (volume) constraint and box constraints are now rewritten respectively as,

$$1/A_{cr} \quad \text{objective function} \quad (28)$$

$$(\text{be.le} \quad dD) - V = 0 \quad \text{linear (volume) constraint} \quad (29)$$

$$b_{min} \leq b_e \leq 1, \quad e = 1, \ldots, Id \quad \text{box constraint} \quad (30)$$

where b_{min} represents a very small positive value (10^{-3} in the examples).

Note that the method just requires the computation of one element of the objective function's generalized gradient set (see equation (26)),

$$\partial_b \left(\frac{1}{\lambda_{cr}} \right) = \{ z, z_e = a_p a_q \left(\langle [J; - \quad] \quad \langle P_q - V_{pq} \; u \right) : a \in R^m, \; \|a\| = 1 \}$$
$$= \{ z = a_p a_q Z_{pq} : a \in R^m, \; \|a\| = 1 \}. \quad (31)$$

This implies solving the equilibrium equation to compute the solution u, solving the generalized eigenvalue problem to compute the eigenvalues λ and eigenvectors ϕ, computing the adjoint displacement v_{pq} satisfying the adjoint equation (24). We stress that BT only needs one element of the generalized gradient set.

The computational implementation considers the objective function and volume constraint scaled as $(1/\lambda)/(1/\lambda_0) = \lambda_0/\lambda$ and $\left(\sum_{e=1}^{Id} b_e f_{ne} dD \right) / V - 1 = 0$.

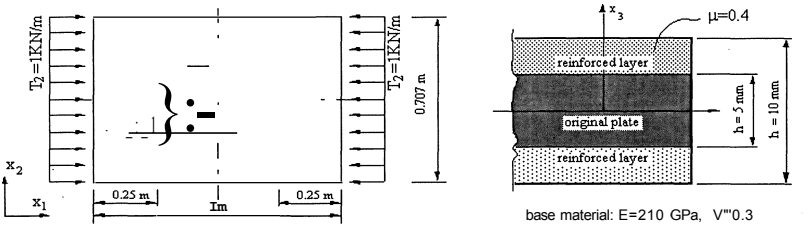

Figure 6. Perturbation regions, loads and geometry

Regions	Increment			Decrenlent		
Perturbed	FFD; 8 = 10->	FFD; 8 = 10-4	Analytical	FFD; 6 = 10-;;	FFD; 8 = 10-4	Analytical
A+B+C+D	152.601	152.715	152.683	-281.884	-281.872	-281.870
A+B	10.459	10.480	10.452	-206. 919	-206.820	-206.824
B+D	76.298	76.378	76.342	-140.956	-140.937	-140.935
B	5.230	5.253	5.226	-103.458	-103.403	-103.412

Table 1. Comparison between finite differences and analytical values

4. Applications

4.1. Sensitivity analysis

This example compares the directional derivative of the critical load factor, obtained from the generalized gradient definition (26), with forward finite difference approximations. We will assume that the critical load factor is strictly positive. Under this condition, the directional derivative in direction b* is given by (see e.g., Clarke, 1982),

$$\frac{d A_{cr}}{d b^*} = -A_{cr}^2 \max_{g \in \partial(1/A_{cr})} (g, b^*) \tag{32}$$

The structure tested is the simply supported plate shown in Fig. 6. The cell base material (see Fig. 3) is isotropic with Young's module E = 210 GPa and Poisson coefficient v = 0.3. The derivatives are computed for positive and negative perturbations in four distinct directions obtained from different perturbations of the regions A, B, C and D identified in Fig. 6. The two reinforcement layers have a uniform material with $b = \mu = 0.4$, $T_2 = 1000$ N/m and the critical load factor has multiplicity two ($\lambda_{cr}1 = A_{cr}2 = 477.05$) for the geometry shown.

Table 1 presents the results obtained. The results show a very good agreement between finite difference values and the analytical derivatives. Also from the different values obtained for negative and positive perturbations, the non-differentiability of the eigenvalues is apparent.

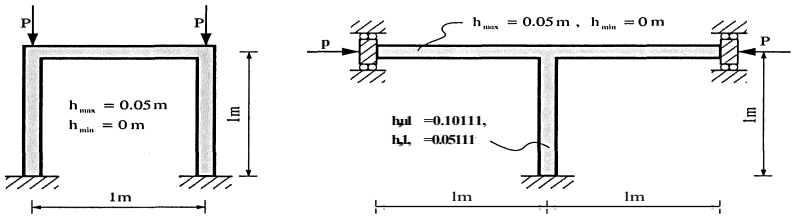

Figure 7. Loads and geometry (case A left, case B right)

4.2. Beam examples

In these examples two cases are presented to show the applicability of the computational model. These cases are show in Fig. 7.

The volume constraint allows for 40% of the maximum thickness and the design process starts with uniform thickness (verifying the volume constraint). The material is isotropic with Young's module $E = 210$ GPa and Poisson coefficient $v = 0.3$. A two-node isoparametric finite element model of 150 elements is used in both cases.

The user-defined BT-code parameters are: FM variable 90% of the initial objective value for the first case and 70% in the second and $LRESET = 5$. This values are adequate for each example but it is not assured that this choice is the optimal one.

The computed critical load factor (first eigenvalue) of the structure for the first and second cases, respectively, are $A_{cr} = 103.2$ and $A_{cr} = 504.3$ for the initial design and $A_{cr} = 160.2$ (55.2% increase) and $A_{cr} = 1683$ (233% increase), respectively, for the final designs after fifty design iterations. The optimal thickness distribution and the evolution of the three lowest eigenvalue, for both cases, are presented in Figs. 8 and 9. Note that for case B the final design has a critical load with multiplicity three ($m = 3$).

4.3. Rectangular plate reinforcement

This example considers the reinforcement of a rectangular plate subjected to inplane forces in one direction. The first case considers a simple supported plate on all boundaries and the other case the plate fixed along one boundary and simply supported along the other ones (see Fig. 10). The total thickness is 10 mm and the thickness of the original plate depends on the ratio of the design layer.

The design process starts with a uniform material distribution and the volume constraint allows for a 20 or 40% surface area increase. The cell base material (see Fig. 3) is isotropic with Young's module $E = 210$ GPa and Poisson

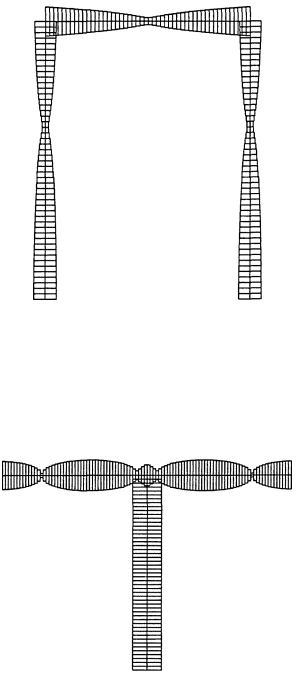

Figure 8. Final design thickness distribution (case A to the left, case B to the right)

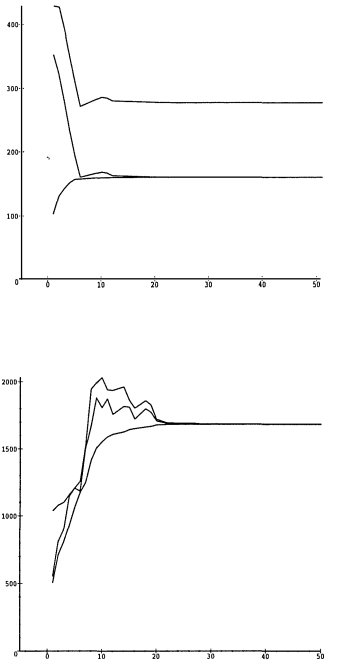

Figure 9. Eigenvalue evolution (case A to the left, case B to the right)

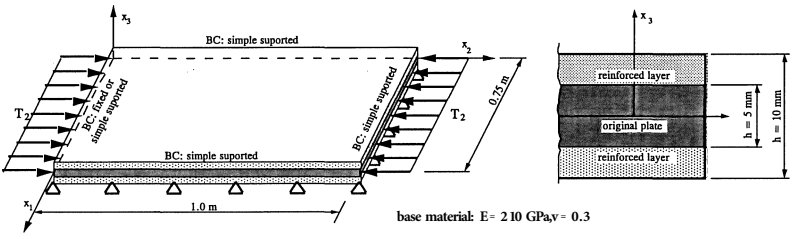

Figure 10. Loads and geometry

	simple supported plate		fixed/simple supported plate	
	initial uniform design	final design	initial uniform design	final design
20% area design material 1/3 thickness design layer	>1 = 513.5 >2 = 555.1	>1 = 628.1 >2 = 628.3	>1 = 531.0 >2 = 693.7	>1 = 732.4 >2 = 732.9
40% area design material 1/3 thickness design layer	>1 = 615.4 >2 = 665.3	>1 = 867.3 >2 = 867.3	>1 = 636.4 >2 = 831.3	>1 = 1010.8 >2 = 1010.9

Table 2. Critical load factors (i^{st} and 2^{nd} eigenvalue)

coefficient v = 0.3. The finite element model uses the eight-node isoparametric elements and has 32 x 24 elements.

The user-defined BT parameters are, for FM variable, 70 or 95% of the initial objective value and $LRESET = 5$. This values are adequate to each example but it is not assure that this choice is the optimal one.

The results are summarized in Table 2 and Figs. 11 and 12. Notice that in all the cases there is an E-double eigenvalue at the final design.

5. Final remarks

The development presented extends the layout design of structures to include a non-smooth critical load criterion. It is applied to the optimal design of plate reinforcements and beam thickness. The problem is solved using a finite element model and a mathematical programming method for non-smooth problems, the Bundle method (Schramm and Zowe, 1992).

The feasibility of the approach presented was substantiated with the resolution of several numerical test examples. The importance of considering the non-smoothness of the problem is established with the good accuracy observed in the computed directional derivatives and, in the optimization examples, a substantial increase was obtained in the critical load of the structures tested.

A limitation in the described model is the issue of the optimal structure sensitivity to geometric imperfections. This is not addressed in this work and using a linear buckling model does not allow for an estimate of this sensitivity. To overcome this limitation a mechanical nonlinear model should be used. Mroz and Haftka (1993) discuss such a model and present sensitivity expressions for shape and size design variables.

One important question in nonsmooth engineering optimization problems relates to the dependability of existent mathematical programming methods. In this issue it was observed that the BT code performed efficiently and can

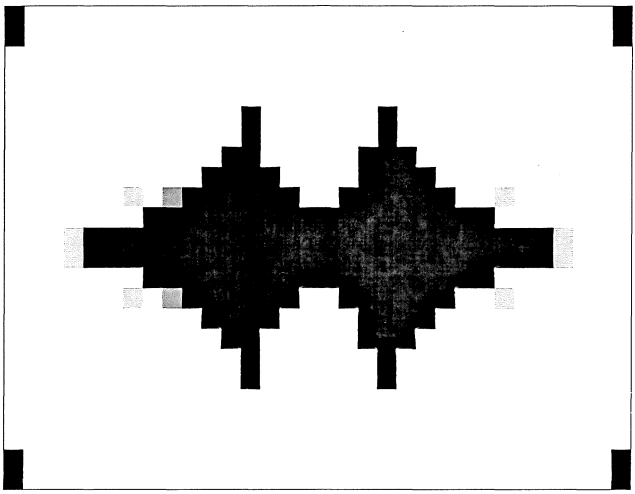

20% Volume Constraint

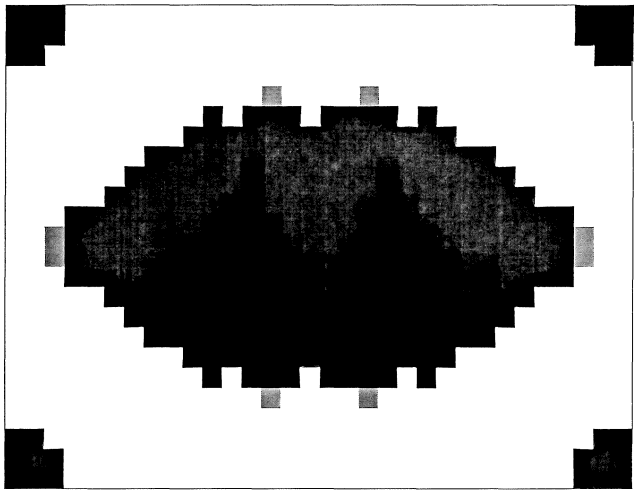

40% Volume Constraint

Figure 11. Simple supported plate reinforcement topologies

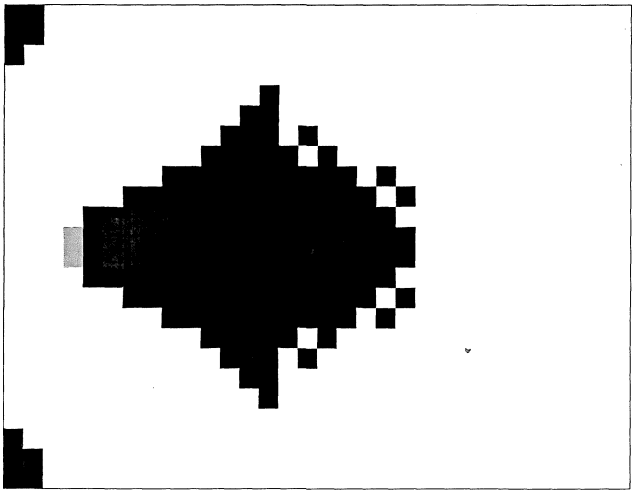

20% Volume Constraint

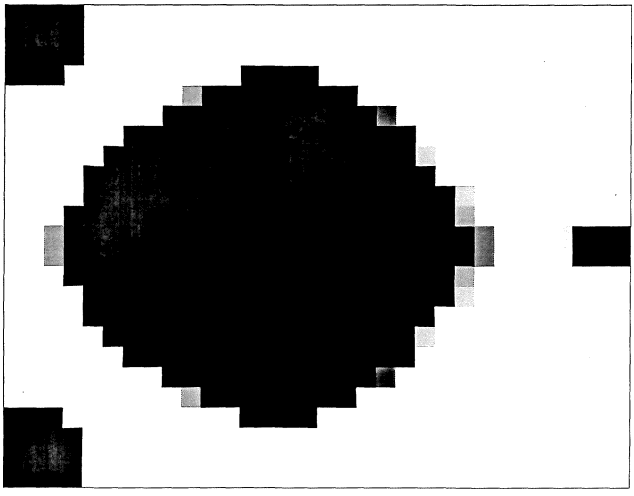

40% Volume Constraint

Figure 12. Fixed/simple supported plate reinforcement topologies

be used as an effective tool in engineering optimization problems. Lately, an intense research effort has been devoted to the study and development of efficient algorithms for non-smooth optimization problems and so it is expected that in the near future these new developments can lead to even more efficient and reliable algorithms.

Acknowledgments

The authors are grateful to Professors M. Bends0e and J.M.Guedes, for very helpful discussions about this subject, and to Dr. M. Kocvara for providing the BT software and for all the help on using the code. This work has been supported by the program PRAXIS XXI and FEDER, project PRAXIS/3/3.1/CTM/10/94.

References

BENDS0E, M.P., MOTA SOARES, C.A., EDS. (1993) *Topology Design of Structures.* Kluwer Academic Publishers, Dordrecht, The Netherlands.

CLARKE, F.H. (1983) *Optimization and Non-Smooth Analysis.* John Wiley and Sons, New York.

DIAZ, A. and KIKUCHI, N. (1993) Solutions to Shape and Topology Eigenvalue Optimization Problems using a Homogenization Method. *International Journal for Numerical Methods in Engineering,* 35, 1487-1502.

FoLGADO, J., RODRIGUES, H. and GUEDES, J.M. (1995) Layout Design of Plate Reinforcement with a Buckling Load Criterion. In: *Structural and Multidisciplinary Optimization* (Eds. Olhoff, N. and Rozvany, G.), Goslar, Germany.

GUEDES, J.M. and KIKUCHI, N. (1990) Preprocessing and Postprocessing for Materials Based on the Homogenization Method .with Adaptive Finite Element Methods. *Comput. Meths. Appl. Mechs. Eng.,* 83, 143-198.

HUGHES, T. (1987) *The Finite Element Method - Linear Static and Dynamic Finite Element Analysis,* Prentice-Hall.

KAM, T.Y. and CHANG, R.R. (1992) Buckling of Shear Deformable Laminated Composite Plates. *Composite Structures,* 22.

MROZ, Z., HAFTKA, R.T. (1993) Design Sensitivity Analysis of Non-Linear Structures in Regular and Critical States. Haslinger, J. (Ed.). Mathematical Methods in Computer Aided Optimal Design. Faculty of Mathematics and Physics, The Charles University. Prague

NEVES, M.M., RODRIGUES, H. and GUEDES, J.M. (1995) Generalized Topology Design of Structures with a Buckling Load Criterion. *Structural Optimization,* 10, 71-78.

NOVOZHILOV, V. (1953) *Foundations of the Nonlinear Theory of Elasticity.* Graylock Press, New York.

0UTRATA, J., SCHRAMM, H. and ZOWE, J. (1991). Bundle Trust Methods: Fortran Code for Nondifferentiable Optimization - User's Guide. Report N269, Universitat Bayreuth, Mathematishes Institut.

RODRIGUES, H., GUEDES, J.M. and BENDS0E, M. (1995) Necessary Conditions for Optimal Design of Structures with a Non-Smooth Eigenvalue Based Criterion. Structural Optimization, 9, 52-56.

SCHRAMM, H. and ZOWE, J. (1992) A Version of the Bundle Idea for Minimizing a Nonsmooth Function: Conceptual Idea, Convergence Analysis, Numerical Results. *SIAM J. Optimization,* 2, 1, 121-152.

SEYRANIAN, A, LUND, E. and 0LHOFF, N. (1994) Multiple Eigenvalues in Structural Optimization Problems. *Structural Optimization,* 8, 207-227.

SOTO, *C.* and DIAZ, A. (1993) On the Modeling of Ribbed Plates for Shape Optimization. *Structural Optimization,* 6, 175-188.

SUZUKI, K. and KIKUCHI, N. (1991) Generalized Layout Optimization of Shape and Topology in Three-Dimension Shell Structures. In: *Geometric Aspects of Industrial Design* (V. Komkov), SIAM, Philadelphia.

VINSON, J.R. and SIERAKOWSKI, R.L. (1987) *The Behavior of Structures Composed of Composite Materials.* Kluwer Academic Publishers, Dordrecht, The Netherlands.